Supporting Information:

Robust Two-Dimensional Bipolar Magnetic Semiconductors by Defect Engineering

Haixia Cheng[⊥†], Jun Zhou[†], Ming Yang[#‡], Lei Shen[§], Jiajun Linghu[†], Qingyun Wu[†¶], Ping Qian*[⊥], Yuan Ping Feng*[† ‡]

[⊥]Department of Physics, University of Science and Technology Beijing, Beijing 100083, China.

[†]Department of Physics, National University of Singapore, Singapore 117411, Singapore.

[‡]Centre for Advanced 2D Materials and Graphene Research Centre, National University of Singapore, Singapore 117546, Singapore.

[#]Institute of Materials Research and Engineering, A*-STAR, 2 Fusionopolis Way, Singapore 138634, Singapore.

[§]Department of Mechanical Engineering & Engineering Science Programme, National University of Singapore, Singapore 117575, Singapore.

[¶]Department of Materials Science and Engineering, National University of Singapore, Singapore 117575, Singapore.

*Correspondence should be addressed to: P. Q (qianping@ustb.edu.cn) and Y.P.F (phyfyp@nus.edu.sg)

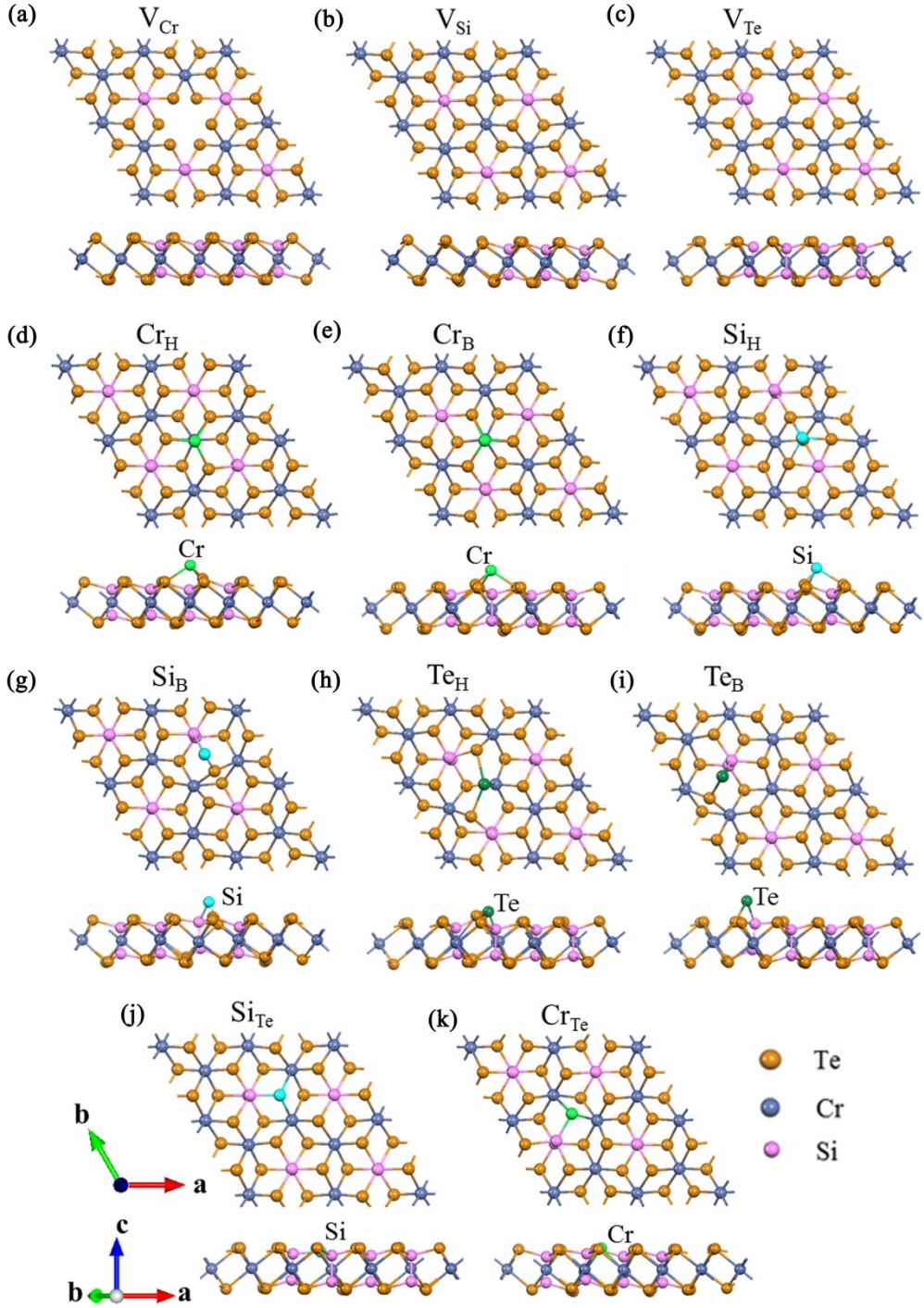

Fig. S1 A top and a side view of optimized geometry of each type of intrinsic defect in $CrSiTe_3$ are shown in (a)-(k). The defect Cr, Si and Te atoms are represented using green, cyan and olive balls, respectively.

Electronic structure of $CrSiTe_3$:Te_{Si} or Te_{Cr}

When the Te_{Si} antisite defect is introduced into $CrSiTe_3$, the system remains a half semiconductor. There are two shallow defect states are induced close to the pristine valence band edge in $CrSiTe_3$:Te_{Si}, and both the band gap and Fermi level are barely changed (see Fig.S2(a)). So, this case belongs to defect tolerance system which may enhance the charge carrier concentration and thereby improve the conductivity [1]. As shown in Fig.S2(b) and (c), these defect states primarily originate from the Te_{Si} s/p_z and in-plane p orbitals (p_x/p_y states) of three nearest Te atoms along with small contribution from the Cr atoms. The total magnetic moment of $CrSiTe_3$ with Te_{Si} defect is 24.153 μ_B, which is almost equal to the value of 24.00μ_B of pristine system due to the defect does not lead to the spin polarized charge.

However, $CrSiTe_3$:Te_{Cr} shows half-metalic features as shown in Fig.S3. The band gap of $CrSiTe_3$:Te_{Cr} is almost same as that in defect free $CrSiTe_3$, and no defect states are observed in the gap of pristine $CrSiTe_3$. The Fermi level moves into the conduction band due to the excess electrons from Te_{Cr}. Clearly, $CrSiTe_3$:Te_{Cr} becomes a half-metal with only spin up channel crossing the Fermi level. The half-metallic gap, labeled as δ in the PDOS shown in Fig.S3(c), is 0.56 eV. The charge density shown in Fig.S3(b) reveals that the energy bands across the Fermi level mainly come from the Cr atoms, indicating that the extra electrons from Te_{Cr} delocalize over host Cr atoms. Similarly delocalized phenomenon has been found in Ga_{Zn} antisite defect for $ZnGa_2O_4$ configurations[2]

and in O vacancy defect for Anatase TiO2(001) Surface [3]. The total magnetic moment of $CrSiTe_3$:Te_{Cr} is 21.91 μ_B, smaller than that in defect free $CrSiTe_3$ (24.00 μ_B) due to the loss of a Cr ion. However, the magnetic moment per Cr ion increases from 3.41 μ_B in defect free $CrSiTe_3$ to 3.43-3.73 μ_B in the defective system due to the gain of electrons on Cr atoms. Table S1 lists the difference of electrons per Cr between $CrSiTe_3$:Te_{Cr} and perfect $CrSiTe_3$ by Bader charge anaysis, further verify our analysis. The electrons of all Cr atoms in Te_{Cr} defect system are increased compare to corresponding in perfect system.

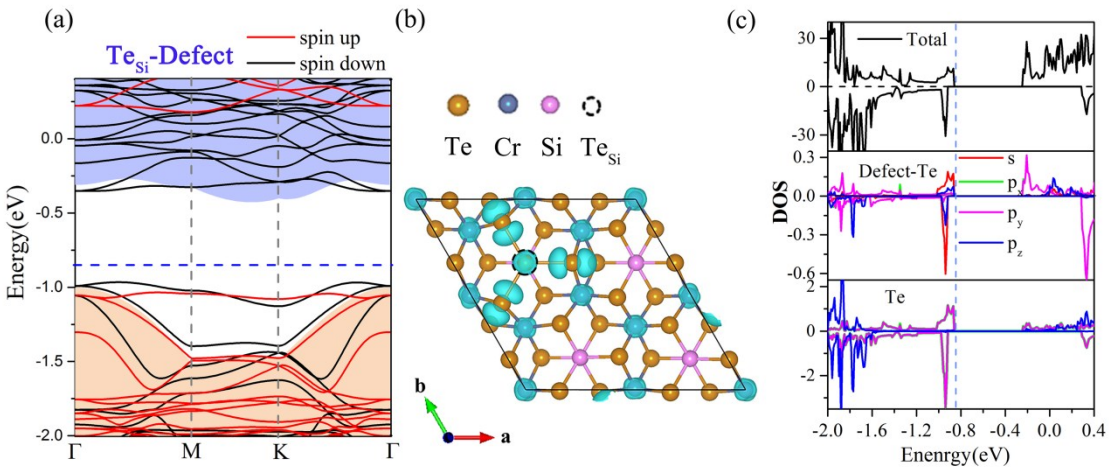

Fig. S2 (a) GGA+*U* calculated spin polarized band structure of $CrSiTe_3$ without and with Te_{Si} defect. Background is band structure of perfect $CrSiTe_3$. All the bands are aligned with the vacuum level. (b) Corresponding partial charge density of defect states in $CrSiTe_3$:Te_{Si} are shown with an isovalue of 0.0025 e/Å^3. (c)Total DOS of $CrSiTe_3$:Te_{Si} and site PDOS of Te_{Si} as well as nearest Te atoms. The blue dashed line divides the occupied and unoccupied states (where the Fermi level is expected to lie).

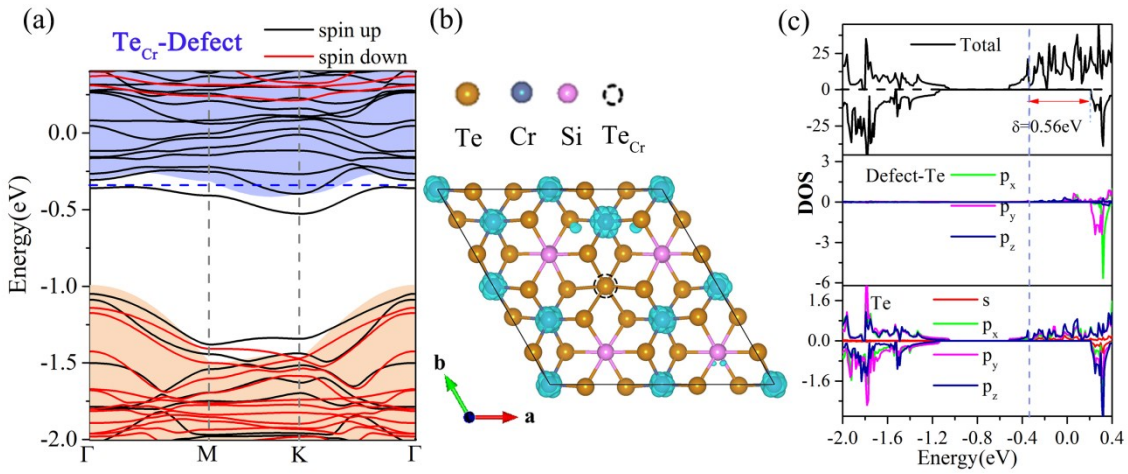

Fig. S3 (a) GGA+*U* calculated spin polarized band structure of $CrSiTe_3$ without and with Te_{Cr} defect. Background is band structure of perfect $CrSiTe_3$. All the bands are aligned with the vacuum level. (b) Corresponding partial charge density of the energy bands across the Fermi level in Te_{Cr} defective system are shown with an isovalue of 0.0025 $e/Å^3$. (c)Total DOS of $CrSiTe_3$:Te_{Cr} and site PDOS of Te_{Cr} as well as nearest Te atoms. The blue dashed line denotes the Fermi level of $CrSiTe_3$:Te_{Cr}.

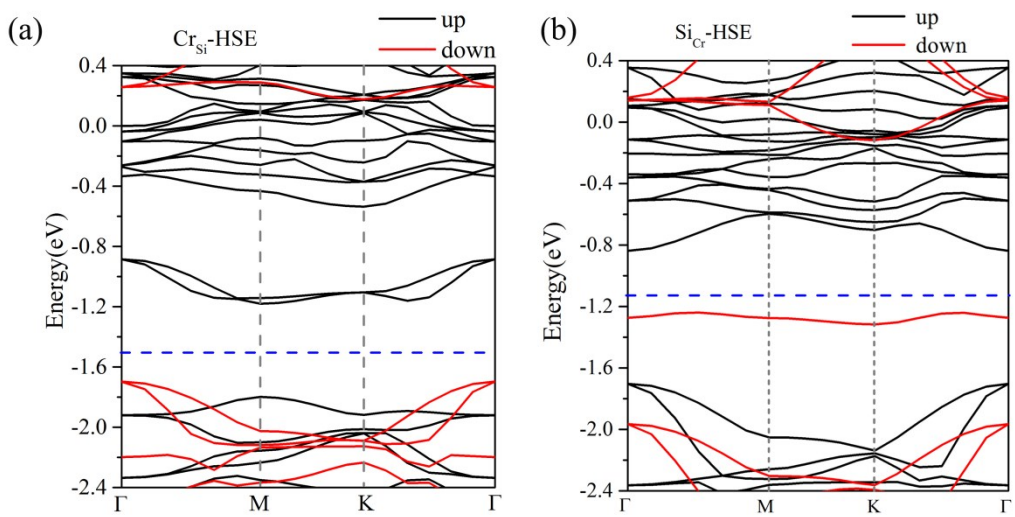

Fig. S4 HSE06 calculated electronic band structure for 3×3×1 monolayer $CrSiTe_3$ with Cr_{Si} defect (a) and Si_{Cr} defect (b). The blue dashed line divides the occupied and unoccupied states (where the Fermi level is expected to lie).

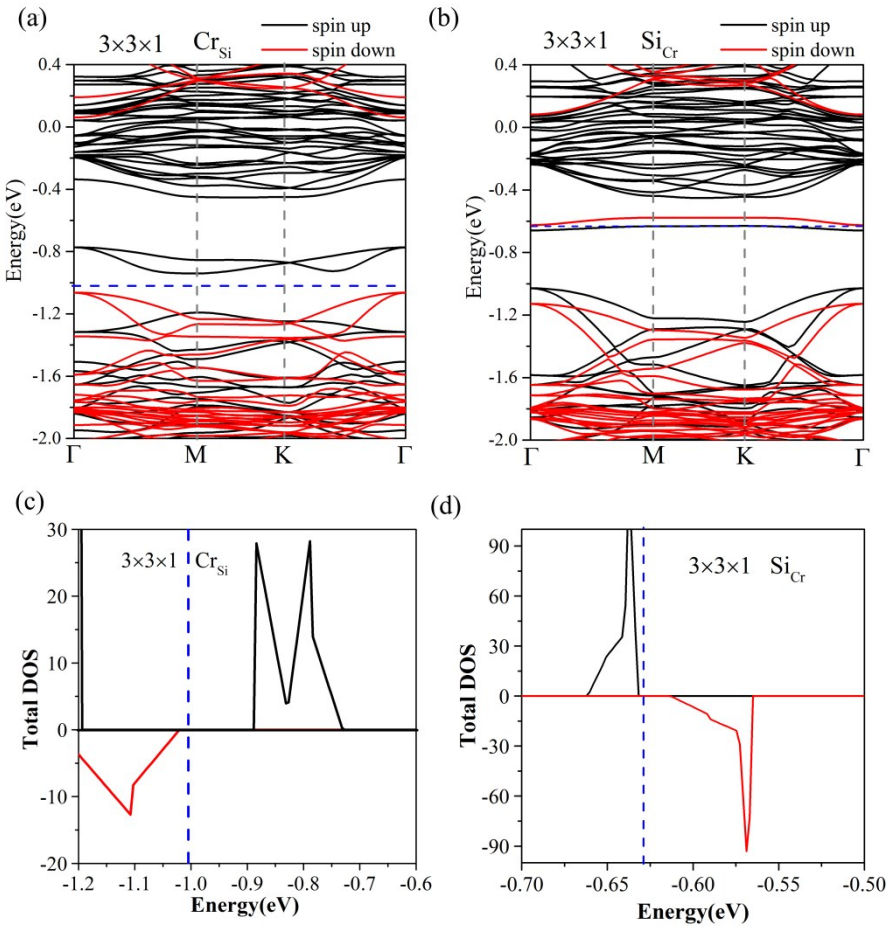

Fig. S5 GGA+*U* calculated electronic properties of 3×3×1 monolayer $CrSiTe_3$ with Cr_{Si} defect and Si_{Cr} defect: (a) and (b) band structure; (c) and (d) local enlarged total DOS. The blue dashed line divides the occupied and unoccupied states (where the Fermi level is expected to lie). The results demonstrate that applying low concentrations of defects do not change the BMS behaviors of Cr_{Si} or Si_{Cr} defective system.

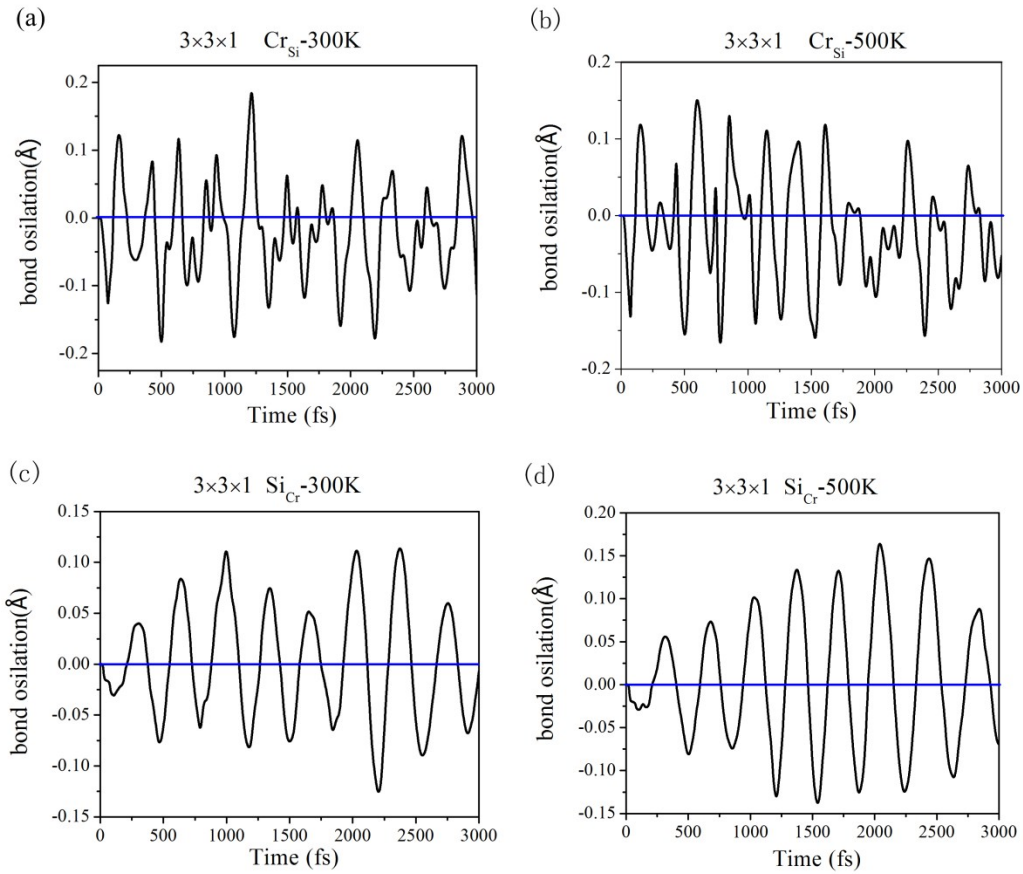

Fig.S6 Bond osilation of defect and nearest Te for both $CrSiTe_3$:Cr_{Si} and $CrSiTe_3$:Si_{Cr} during MD simulation at the temperature of 300K and 500K, respectively.

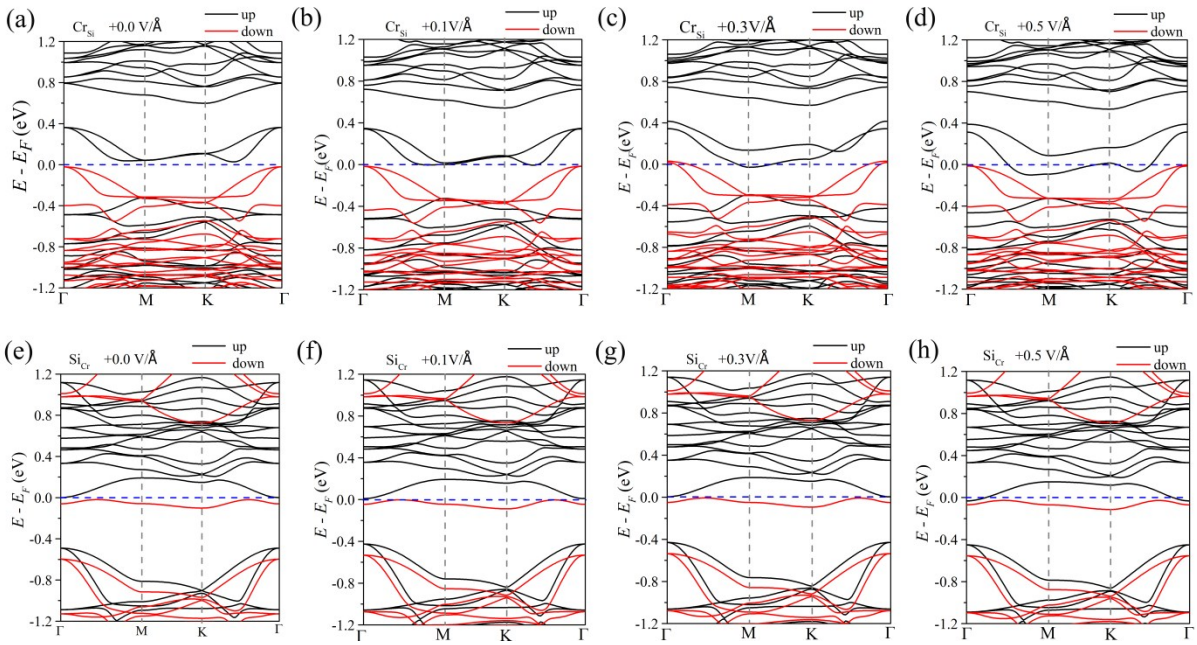

Fig.S7 GGA+U calculated band structure of (a)-(d) $CrSiTe_3$:Cr_{Si} and (e)-(h) $CrSiTe_3$:Si_{Cr} without and with electric field.

Table S1 Calculated the difference value of electrons for Cr atoms between Te_{Cr} defect $CrSiTe_3$ system and pristine system based on Bader charge analysis. The unit of the charge is *e*, for which positive values indicate electron increase. Cr1-Cr7 refer to all Cr atoms.

	Cr1	Cr2	Cr3	Cr4	Cr5	Cr6	Cr7
Charge change	0.0204	0.0294	0.0196	0.0129	0.0075	0.0067	0.0572

Table S2 GGA+U calculated band gap (E_g), spin flip energy in the valence band (Δv) and in the conduction band (Δc), respectively, for both defected $CrSiTe_3$:Cr_{Si} and $CrSiTe_3$:Si_{Cr} with various supercell sizes.

Cr_{Si}	E_g (eV)	Δv (eV)	Δc (eV)
2×2×1	0.060	0.300	1.281
2×3×1	0.062	0.195	1.134
3×3×1	0.138	0.176	0.991
3×4×1	0.157	0.043	0.996
4×4×1	0.205	0.043	0.962
Si_{Cr}	**E_g (eV)**	**Δv (eV)**	**Δc (eV)**
2×2×1	0.020	0.579	0.722
2×3×1	0.020	0.549	0.126
3×3×1	0.021	0.541	0.158
3×4×1	0.048	0.486	0.143
4×4×1	0.062	0.476	0.129

References

1. X. Wen, Y. Feng, S. Huang, F. Huang, Y.-B. Cheng, M. Green and A. Ho-Baillie, *J. Mater. Chem. C*, 2016, **4**, 793-800.

2. A. De Vos, K. Lejaeghere, D. E. Vanpoucke, J. J. Joos, P. F. Smet and K. Hemelsoet, *Inorg. Chem.*, 2016, **55**, 2402-2412.

3. Y. Shi, H. Sun, M. C. Nguyen, C. Wang, K. Ho, W. A. Saidi and J. Zhao, *Nanoscale*, 2017.